

Effect of changing reagent energy on reaction dynamics. XI. Dependence of reaction rate on vibrational excitation in endothermic reactions $\text{HX}(v \text{ reag}) + \text{Na} \rightarrow \text{H} + \text{NaX} (\text{X} = \text{F}, \text{Cl})$

F. E. Bartoszek, B. A. Blackwell, J. C. Polanyi, and J. J. Sloan

Citation: *The Journal of Chemical Physics* **74**, 3400 (1981); doi: 10.1063/1.441493

View online: <http://dx.doi.org/10.1063/1.441493>

View Table of Contents: <http://scitation.aip.org/content/aip/journal/jcp/74/6?ver=pdfcov>

Published by the [AIP Publishing](#)

Articles you may be interested in

Statostate dynamics of $\text{H} + \text{HX}$ collisions. I. The $\text{H} + \text{HX} \rightarrow \text{H}_2 + \text{X}$ ($\text{X} = \text{Cl}, \text{Br}, \text{I}$) abstraction reactions at 1.6 eV collision energy

J. Chem. Phys. **90**, 4795 (1989); 10.1063/1.456574

Comparison of reagent translation and vibration on the dynamics of the endothermic reaction $\text{Sr} + \text{HF}$

J. Chem. Phys. **72**, 6250 (1980); 10.1063/1.439038

Effect of changing reagent energy. X. Vibrational threshold energies for alternative reaction paths $\text{HF}(v) + \text{D} \rightarrow \text{F} + \text{HD}$ and $\rightarrow \text{H} + \text{DF}$

J. Chem. Phys. **69**, 933 (1978); 10.1063/1.436610

Effect of reagent vibrational excitation on the rate of a substantially endothermic reaction; $\text{HCl}(v' = 1-4) + \text{Br} \rightarrow \text{Cl} + \text{HBr}$

J. Chem. Phys. **59**, 6679 (1973); 10.1063/1.1680052

Rates of the Endothermic Reactions $\text{HCl} + \text{X}$ ($\text{X} = \text{I}, \text{Cl}$) as a Function of Reagent Vibration, Rotation, and Translation

J. Chem. Phys. **51**, 5716 (1969); 10.1063/1.1672004



Effect of changing reaction reagent energy on reaction dynamics. XI. Dependence of reaction rate on vibrational excitation in endothermic reactions $\text{HX}(v_{\text{reag}}) + \text{Na} \rightarrow \text{H} + \text{NaX}(\text{X} \equiv \text{F, Cl})$

F. E. Bartoszek,^{a)} B. A. Blackwell,^{b)} J. C. Polanyi, and J. J. Sloan^{c)}

Department of Chemistry, University of Toronto, Toronto, Canada M5S 1A1
(Received 27 August 1980; accepted 7 November 1980)

The chemiluminescence depletion (CD) method has been applied to two endothermic reactions to obtain approximate relative rates of reaction $k_{\text{endo}}(v_{\text{reag}})$ out of specified reagent vibrational levels v_{reag} for a range of vibrational energies V_{reag} extending to well above the energy barrier Q . The reactions were (1) $\text{HCl}^{\dagger}(v_{\text{reag}} = 1-4) + \text{Na} \rightarrow \text{H} + \text{NaCl}(Q = -4.2 \text{ kcal mole}^{-1}, Q_c = -10 \text{ kcal mole}^{-1})$ and (2) $\text{HF}^{\dagger}(v_{\text{reag}} = 1-5) + \text{Na} \rightarrow \text{H} + \text{NaF}(Q = -12 \text{ kcal mole}^{-1}, Q_c = -18 \text{ kcal mole}^{-1})$. The major finding is that for high V_{reag} , with over 90% of the reagent energy present as vibration, the collision-efficiency for both reactions is approximately unity. From this we conjecture that the barrier crest is "late," with little extension into the entry valley (type IIS). The reactive cross sections exceed by an order of magnitude the (large) cross section of several Å^2 obtained in part VI for endothermic reactions $\text{HX}^{\dagger} + \text{Y}$ (e.g., $\text{HF}^{\dagger} + \text{Cl}$). The salient difference is likely to be the fact that the present reactions involve a switch from covalent to ionic bonding. To within experimental error the same absolute vibrational energy in either HCl^{\dagger} or HF^{\dagger} gives rise to the same absolute cross section for reaction with Na.

I. INTRODUCTION

The effect of systematic changes in reagent vibration, rotation, and translation (V, R, T) on reaction rate k and product energy distribution—i.e., on reaction dynamics—is a lively field for theory and experiment.¹ The series of experimental studies of which the present work forms a part began with an investigation of the effect of T_{reag} on V_{prod} , R_{prod} , and T_{prod} (subscripts indicate reagent and product energies) using a seeded supersonic jet to vary T_{reag} and the arrested relaxation infrared chemiluminescence method to obtain V_{prod} , R_{prod} , and T_{prod} .² The technique common to all papers in this series has been the recording of chemiluminescence in the infrared. Use has been made of the methods of fluorescence depletion (FD)³ and chemiluminescence depletion (CD)^{3,4} in order to measure $k(V_{\text{reag}}, R_{\text{reag}})$ over a wide range of V and R .⁵

The present work has to do with the effect of reagent vibration (in the absence of enhanced reagent rotation and translation) on the rates of endothermic reactions. For endothermic exchange reactions $\text{AB} + \text{C} \rightarrow \text{A} + \text{BC}$ (we write $\text{A} + \text{BC} \rightarrow \text{AB} + \text{C}$ in the exothermic direction, and $\text{AB} + \text{C} \rightarrow \text{A} + \text{BC}$ to indicate an endothermic exchange reaction^{1(a)}) in which a covalent bond is being broken and another covalent bond is being formed, it was suggested some time ago that the barrier to reaction would be "late," i.e., it would have its crest along the coordinate of separation, corresponding to extension of the bond AB under attack, and that as a consequence vibrational excitation in AB, V_{reag} , would be much more effective than T_{reag} in enhancing the reactive cross section.⁶ The most detailed experimental evidence for this

proposition is embodied in the so-called "endothermic triangle plots" which record $k_{\text{endo}}(V_{\text{reag}}, R_{\text{reag}}, T_{\text{reag}})$ obtained from the application of microscopic reversibility to rate constants $k_{\text{exo}}(V_{\text{prod}}, R_{\text{prod}}, T_{\text{prod}})$ obtained in infrared chemiluminescence studies.⁷ The procedure used for obtaining k_{endo} from k_{exo} has been checked in detail by means of a Monte Carlo trajectory study in which $k_{\text{endo}}(V_{\text{reag}}, R_{\text{reag}}, T_{\text{reag}})$ was obtained by direct calculation as well as by the application of microscopic reversibility to $k_{\text{exo}}(V_{\text{prod}}, R_{\text{prod}}, T_{\text{prod}})$ for the same potential-energy surface.⁸ It should be noted that these data apply to the effects of a redistribution of a constant total energy between $V_{\text{reag}}, R_{\text{reag}},$ and T_{reag} , close to the threshold energy for endothermic reaction. The largest increase of k_{endo} with increasing V_{reag} , and correspondingly decreasing T_{reag} , is found for R_{reag} greatly in excess of thermal rotational excitation. It is then found that V_{reag} is orders-of-magnitude more effective in promoting endothermic reaction than in T_{reag} —the actual values can be read off the endothermic triangle plots.

In addition to the trajectory studies on stereotype "early" and "late" barrier-crest surfaces (termed "type I" and "type II," respectively),⁸ a number of trajectory studies have been made on endothermic surfaces with various types of late barriers. The reactive cross sections, and hence in the great majority of cases the detailed rate constants $k_{\text{endo}}(V_{\text{reag}}, R_{\text{reag}}, T_{\text{reag}})$, were found to rise much more steeply with increase in reagent vibration than with the same increase in reagent translation.⁹⁻¹¹ The requirement for a sufficient translational energy to carry the system up that part of the energy barrier which extended into the approach coordinate for endothermic reaction was noted¹¹ (in all these theoretical studies^{6,9-11} it was the barrier crest, not the entire energy barrier, that was "early" or "late"). The criterion used for separating the approach coordinate from the retreat coordinate was the location, along the minimum-energy path, of the position of *equal bond extension* (relative to equilibrium bond distance), in the

^{a)} Present address: Department of Chemistry, Stanford University, Stanford, CA 94305.

^{b)} Present address: Division of Biology, National Research Council, 100 Sussex Drive, Ottawa, Ontario, Canada K1A 0R6.

^{c)} Present address: Division of Chemistry, National Research Council 100 Sussex Drive, Ottawa, Ontario, Canada K1A 0R6.

bond that is dissolving and the bond that is forming.^{6(c)} Other workers have divided energy release in the exothermic direction (or energy consumption in the endothermic direction) into energy released (or consumed) before and after the point of *maximum curvature* in the minimum energy path.^{12,13} Recently it has been shown that the two criteria are equivalent.^{14(a)}

If a "late" barrier crest is designated type II,⁶ then surface IIG (G ≡ "gradual," denoting a gradual rise to the late barrier crest) utilizes reagent translation—the disfavored degree of freedom—more effectively than does IIS (S ≡ "sudden").¹⁴ Notwithstanding these refinements, the broad generalization that a late barrier crest has the consequence $S_r(V_{\text{reag}}) > S_r(T_{\text{reag}})$ (where S_r is the reactive cross section and the inequality is intended to indicate that a given reagent energy gives a larger cross section when vested in vibration than in translation) retains its usefulness.

Two theoretical propositions should be distinguished: (a) Substantially endothermic reactions have late barrier crests, and (b) late barrier crests correlate with a more rapid rise for $S_r(V_{\text{reag}})$ than $S_r(T_{\text{reag}})$, with equivalent energy in V_{reag} or T_{reag} . The first of these propositions has a demonstrated general basis only for covalent-covalent reactions (for this case we have, in addition, some basis for a sufficient criterion of "substantial" endothermicity^{7(c)}), but may apply to other families of reaction. One of the earliest experimental demonstrations of the superior effectiveness of V_{reag} over T_{reag} was for the endothermic ion-molecule reaction $\text{H}_2^+ + \text{He} \rightarrow \text{H} + \text{HeH}^+$. Reagent vibration was found to be roughly an order-of-magnitude more effective than translation in promoting reaction.¹⁵ *Ab initio* calculations indicated that the potential-energy surface for this 3-electron system had its barrier crest displaced into the exit valley,^{16,17} lending support to the correlation made under (b) above, and thus raising the possibility of a wider application for generalization (a).

A second case in which $S_r(V_{\text{reag}})$ was clearly shown to increase more rapidly than $S_r(T_{\text{reag}})$, by about an order of magnitude, was the reaction $\text{HCl}(v=0, 1) + \text{K} \rightarrow \text{H} + \text{KCl}$.¹⁸ Proposition (b) above would lead us therefore, to infer a later barrier crest. Proposition (a) is somewhat in doubt since the reaction involves a switch from a covalent to an ionic potential-energy surface—see, however, recent theoretical studies of the energy-surfaces for other such reactions $\text{HX} + \text{M}$ [M ≡ alkali metal] which give a late barrier crest for the endothermic cases,¹⁹⁻²¹ as well as the findings for this family of reactions reported in this paper. Proposition (a) is, moreover, of little value if the reaction is only marginally endothermic; for $\text{HCl} + \text{K}$ the endothermicity is $-\Delta H_0^\circ \equiv Q \approx 1.5$ kcal mol⁻¹.¹⁸

For *substantially* endothermic reactions ($Q > 10$ kcal mol⁻¹^{7(c)}) involving covalent-covalent energy surfaces, triangle plots have been published giving $k_{\text{endo}}(V_{\text{reag}}, R_{\text{reag}}, T_{\text{reag}})$ for (i) $\text{HCl}(v=1-4) + \text{I} \rightarrow \text{Cl} + \text{HI}$ ($Q = -31.7$ kcal mol⁻¹; note that $Q \equiv -\Delta H_0^\circ$ so that $Q > 0$ for exothermic reaction, and < 0 for endothermic^{7(a)}), (ii) $\text{HCl}(v=1-4) + \text{Cl} \rightarrow \text{H} + \text{Cl}_2$ ($Q = -45.1$ kcal mol⁻¹),^{7(a)} (iii) $\text{HF}(v=1-3) + \text{H} \rightarrow \text{F} + \text{H}_2$ ($Q = -31.5$

kcal mol⁻¹),^{7(b)} (iv) $\text{HF}(v=1-3) + \text{D} \rightarrow \text{F} + \text{HD}$ ($Q = -31.1$ kcal mol⁻¹),^{7(c)} and (v) $\text{DF}(v=1-4) + \text{H} \rightarrow \text{F} + \text{HD}$ ($Q = -32.8$ kcal mol⁻¹).^{7(c)} As noted above, the endothermic triangle plots give k_{endo} for constant total reagent energy; the effect of increase in energy vested in any one or more degrees of freedom, $V_{\text{reag}}, R_{\text{reag}}$ or T_{reag} , is therefore recorded for constant $V_{\text{reag}} + R_{\text{reag}} + T_{\text{reag}}$.

Infrared-luminescence depletion methods, FD and CD above, have proved to be useful in obtaining $k_{\text{endo}}(V_{\text{reag}})$ ^{3,4} and $k_{\text{endo}}(R_{\text{reag}})$, without an inherent restriction on the total reagent energy, up to energies greatly in excess of the endothermic barrier energy. The procedure in, for example, chemiluminescence depletion (CD) which will be used once again in the present study, is to produce vibrationally excited AB^\dagger in a prior chemical reaction $\text{A} + \text{BC}$, termed the "prereaction." The AB^\dagger emits in the infrared from a wide range of v, J states of AB^\dagger . Provided that the dominant path for removal of AB^\dagger is reaction, $\text{AB}^\dagger + \text{D}$, and not deactivation (which would be seen to populate adjacent lower states), the relative rates of reaction $k(v, J)$ are given by the relative magnitudes of the fractional depletions, $-\Delta N(v, J)/N(v, J)$, for each individual reagent vibrotational state.

The CD method has been examined in detail and applied (with various prereactions and relative flows of prereagents) to the covalent-covalent reactions, $\text{HCl}(v=1-4) + \text{Br} \rightarrow \text{Cl} + \text{HBr}$ ($Q^\ddagger \approx -16.5$ kcal mol⁻¹), $\text{HF}(v=1-6) + \text{Cl} \rightarrow \text{F} + \text{HCl}$ ($Q^\ddagger \approx -34$ kcal mol⁻¹), and $\text{HF}(v=1-6) + \text{Br} \rightarrow \text{F} + \text{HBr}$ ($Q^\ddagger \approx -49$ kcal mol⁻¹).^{4(b)} The symbol Q^\ddagger denotes the total endothermic barrier, $-\Delta H_0^\circ + E_a$, where E_a is the barrier to the reverse (exothermic) reaction.^{4(b)} All three of these reactions fall under the heading of "substantially endothermic" covalent-covalent reactions. All three reactions (irrespective of prereaction) exhibited a threshold energy for reaction at the vibrational level v with energy $V \approx Q^\ddagger$. Five different methods (all of them approximate) were used to place $k_{\text{endo}}(V_{\text{reag}})$ for $\text{HCl}(v) + \text{Br} \rightarrow \text{Cl} + \text{HBr}$ on an absolute scale; all led to reactive cross sections $S_r(v=4) = 1-4 \text{ \AA}^2$. Similar S_r were obtained for $v=6$ in $\text{HF}(v) + \text{Cl}$ and $\text{HF}(v) + \text{Br}$. Since the reagent translation and rotation was thermal (300 K), the finding was that very high collision efficiencies, approaching 0.1, could be obtained by placing some 96% of the reagent energy in the degree of freedom that theory [propositions (a) and (b) above] would predict to be the preferred type of motion for barrier crossing.

Very recently the crossed molecular beam approach has been successfully applied in Zare's laboratory to the measurement of $S_r(V_{\text{reag}})$ and also $S_r(T_{\text{reag}})$ in a substantially endothermic reaction; the reaction was $\text{HF}(v=0-1) + \text{Sr} \rightarrow \text{SrF} + \text{H}$, $Q = -6.4 \pm 1.6$ kcal mol⁻¹.²² It has been shown in previous work from the same laboratory that laser excitation of HF from $v=0$ to $v=1$ increased the rate of this reaction by at least four orders-of-magnitude.²³ A comparable increase in collision energy can be obtained by using a seeded supersonic jet of Sr. Reagent vibration was found to be more effective than reagent translation, but only by a modest factor in the range 1-10x.²²

The present work, in common with the study per-

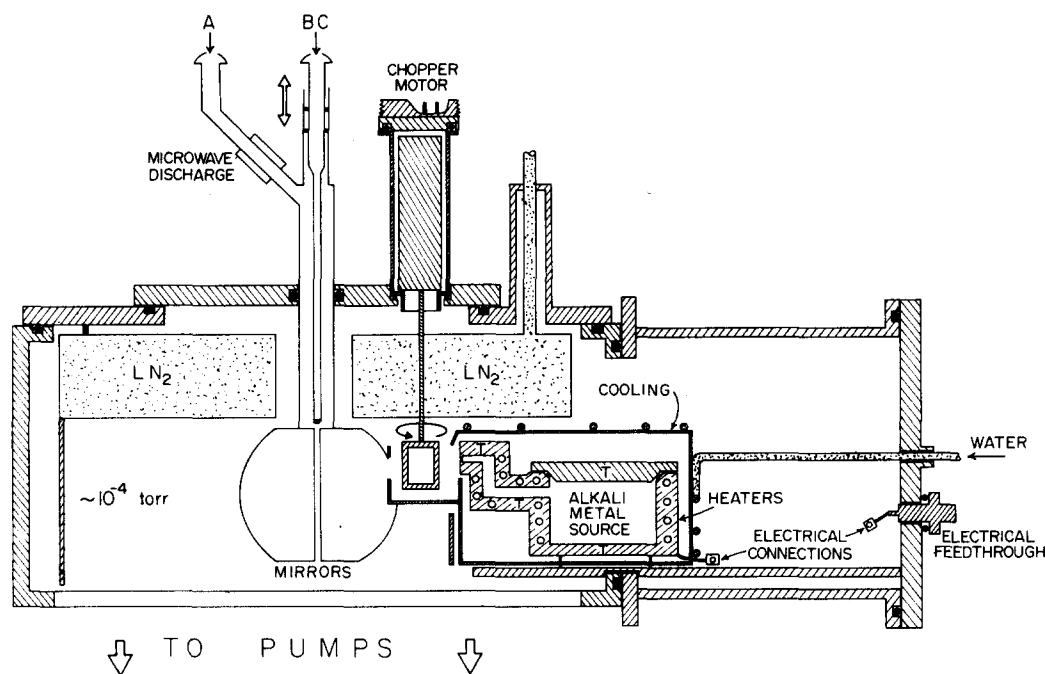
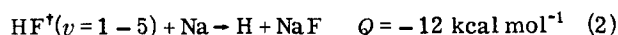


FIG. 1. Cross sectional view of the reaction vessel with the sodium oven in place. The walls surrounding the reaction zone are liquid nitrogen cooled. The "prereagents," A and BC enter through the quartz inlet system at the top, and the chemiluminescence is collected by the gold-coated mirrors of the Welsh cell located below the prereactor. The sodium oven rests on stainless steel pins and is surrounded by a water-cooled shield. Thermocouple locations are marked "T."

formed by Zare and co-workers^{22,23} deals with substantially endothermic reactions between metal atoms and hydrogen halides, i.e., covalent \rightarrow ionic energy surfaces. It may be significant, as Gupta *et al.*²² observe, that in $\text{HF} + \text{Sr}$ the reacting entities can (in principle) form a stable intermediate, HSrF , thus raising the possibility of an intermediate complex *en route* from reactants to products. The potential-energy surface for the different class of metal atom reactions studied in this laboratory $\text{HX} + \text{M}$, $\text{X} \equiv \text{Cl}, \text{F}$, and $\text{M} \equiv$ an alkali metal atom, has been the subject of a number of theoretical studies¹⁹⁻²¹ since we embarked on our experiments.^{5,25} The computed potential energy surfaces are of "type II," i.e., they have late barrier crests, and since they are free of potential wells they would be consistent with direct reaction. The chemiluminescence depletion method has been applied, in the work reported below, to the study of the detailed rate constants $k_{\text{endo}}(v_{\text{reag}})$ for the reactions



(the dagger indicates vibrational excitation in the ground electronic state). The endothermicities without inclusion of zero point vibrational energy are $Q_c = -10 \text{ kcal mol}^{-1}$ for $\text{HCl}^\dagger + \text{Na}$, and $Q_c = -18 \text{ kcal mol}^{-1}$ for $\text{HF}^\dagger + \text{Na}$, hence the potential-energy surfaces can be characterized as "substantially endothermic."

A preliminary report regarding $k_{\text{endo}}(v_{\text{reag}})$ has already appeared²⁵ as also has a detailed report on the effect of changing reagent energy on the rate constant, $k_{\text{endo}}(J_{\text{reag}})$.⁵ Our major finding in regard to $k_{\text{endo}}(v_{\text{reag}})$ ²⁵ is that for high V_{reag} , with $\sim 93\%$ of the reagent energy present as vibration (4% translation, 3% rotation) the

collision efficiency for reaction is ~ 1 ; i.e., vibration is extremely efficient in bringing about reaction. This finding is confirmed in the present study. Such a large reactive cross section in the absence of substantial reagent translation suggests a surface of type II S (late barrier crest II, preceded by a relatively sudden rise S; see above). The "harpooning" model, in which reaction occurs when the system switches from a covalent potential, $\text{HX}^\dagger + \text{M}$, to an ionic one, $\text{HX}^- + \text{M}^+$ provided a simple rationale for the large reactive cross-section. Finally, we made a comparison of the reaction rate, and vibrational energy dependence of the rate for the two reactions $\text{HX} + \text{Na}$ at high reagent vibration; there was no detectable difference, indicative of similar surface topology.

II. EXPERIMENTAL

The reaction vessel has been described previously^{26,27} and consequently only the essential details will be given here.

A schematic diagram of the "arrested relaxation" reaction vessel with the alkali metal oven in place is shown in Fig. 1. The reaction vessel itself was a monel box, into which was inserted a copper baffle. This baffle had a reservoir at the top through which a continuous stream of liquid nitrogen flowed. A copper skirt 1/8 in. thick was hard soldered around the edge of this circular reservoir and the skirt (cooled by conduction from the reservoir) surrounded the reaction zone. This cold surface cryopumped condensable gases (e.g., Cl_2 , HI , etc.) and also deactivated vibrationally excited molecules to the ground state. An additional cold surface was provided by an NRC Chevron cold baffle

filled with liquid nitrogen; this baffle was located directly below the reaction zone.

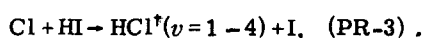
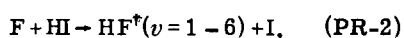
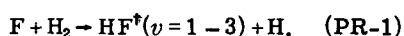
The gases entered through the concentric quartz inlet system, described as the "prereactor," at the top. The atomic species A (Fig. 1) was formed in a continuous microwave discharge (80 W, 2450 MHz) in the arm on the left (using CF_4 for F atoms or Cl_2 for Cl atoms). The prereactor was internally coated with phosphoric acid to minimize wall recombination of the atoms (in the case of Cl atoms) and to protect the prereactor from attack (in the case of F atoms).

The molecular species entered through the 3 mm i. d. central tube and was injected laterally into the stream of atoms coming from a 20 mm i. d. outer tube at the bottom of the prereactor. The prereagents reacted in the high pressure region ($\sim 10^{-1}$ – 10^{-2} Torr depending upon the prereagent flow that was selected) at the lower end of the prereactor to form a distribution of vibrationally excited reagent. This distribution could be varied by altering the reagent flow, or prereactor geometry (in the latter case the central tube of the prereactor would be withdrawn or lowered with respect to the concentric inlet).

The vibrationally excited reagent expanded into the low pressure region ($\sim 10^{-3}$ – 10^{-4} Torr) below the prereactor; this spray intersected, at right angles, a diverging beam of sodium atoms emerging from the oven. The beam of Na atoms was modulated by a "barrel" chopper placed directly in front of the nozzle. The infrared emission from the vibrationally excited reagent was collected by the gold-coated mirrors of the Welsh cell,²⁸ located just below the prereactor (a cross section of the Welsh cell is illustrated in Fig. 1). Infrared emission was then focused onto the entrance optics of an Interactive Technology (CT-103) 1 m grating spectrometer. The infrared intensity was monitored by means of a liquid nitrogen cooled PbS detector (Infrared Industries).

Two spectral traces were recorded simultaneously. A lock-in amplifier (PAR HR-8) was tuned to the modulation frequency (~ 100 Hz) of the total emission from the reaction vessel; the signal from this amplifier gave the spectrum of the vibrationally excited reagent formed in the prereactor. A second lock-in amplifier (PAR 124) was tuned to the ~ 17 Hz modulation frequency of the barrel chopper in front of the Na oven; the signal from this amplifier gave directly the change in intensity of each ν , J line due to the presence of Na. The reason for using this method was to improve signal-to-noise ratios and to minimize the effects of variations in the flows of reagents. The modulation frequencies were chosen so that neither frequency was a multiple of the other, or of 60 Hz. For further details concerning this method, see Ref. 27(a).

The three prereactions that were used were



The gases were supplied by Matheson of Canada. The

CF_4 (99.7%), H_2 (99.999%), and Cl_2 (UHP, 99.9%) were used directly from the cylinders without further purification. The HI (98%) was condensed into a liquid nitrogen cooled trap. The frozen gas was allowed to warm to the liquid state, then refrozen using liquid nitrogen; residual (noncondensable) gases were removed by pumping on the solid. This procedure was repeated a second time to ensure that there was no noncondensable gas trapped in a solid HI matrix. Finally, the HI was allowed to warm again to the liquid state and a chloroform slush (210 K) was placed around the trap. After equilibration, the HI vapor pressure remained constant at 150 Torr. A constant forepressure of noncorrosive gases was maintained by a Matheson Model 40 vacuum regulator. The gas flows were measured using Fisher-Porter Tri-Flat flow meters; the flows are listed in Table I. Sodium metal (Fisher Certified Reagent), in hermetically sealed shipping tins, was used. Sodium packed under kerosene was no longer used following trial experiments since solvents employed to remove the kerosene remained on the sodium in the oven and tended to pyrolyze in the nozzle, clogging the opening.

The sodium oven was a standard two chamber source, based on the design given by Sholeen.²⁹ The oven is described in detail in Ref. 30.

Temperatures were measured using the chromel-alumel thermocouples (Leeds and Northrup). These temperatures could be used to calculate the sodium vapour pressure and thus the flow rate (assuming viscous flow^{27(a)}). The flow rate of sodium at an oven temperature of ~ 500 °C was 10–15 $\mu\text{mol s}^{-1}$. A second method to estimate the flow was based on the amount of sodium metal that the oven contained before and after an experiment. This difference gave the number of moles of sodium vapourized. Since the total time that the sodium was flowing was known the flow rate could be obtained. This flow rate agreed well with the rate calculated by the first method.

As mentioned above, two spectral traces were recorded simultaneously—the intensity of each ν , J line [$I(\nu, J)$] and the change in intensity due to the reaction of sodium with the excited hydrogen halide [$-\Delta I(\nu, J)$].

TABLE I. Experimental flows ($\mu\text{mol s}^{-1}$).

Pre-reaction	CF_4	H_2	CH_3I	HI	Cl_2	Na	Figure
(a) HCl + Na							
Cl + HI				42	158	1	3 □
Cl + HI				30	77	1	3 △
Cl + HI				65	163	1	3 ◇
Cl + HI				61	114	10	3 ○
(b) HF + Na							
F + H_2	25	32				10	4 ◇
F + CH_3I	30		30			10	4 +
F + HI	29			45		5	4 △
F + HI	35			37		10	4 ○
F + HI	37			53		5	4 □

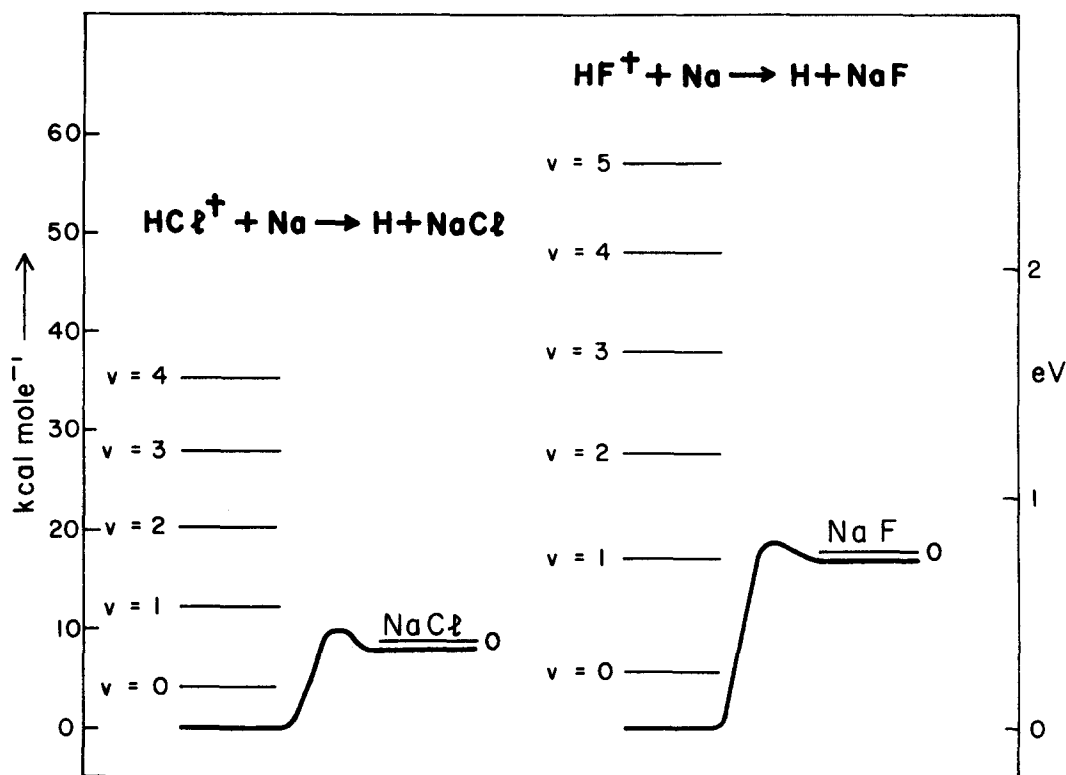


FIG. 2. Vibrational energy levels and schematic potential energy profiles for the endothermic reactions HX^\dagger ($X = F, Cl$) + Na. The potential energy profile is drawn without inclusion of zero point energy. The reagent and product lines marked "O" indicate the magnitude of the zero point energies. The endothermicities without inclusion of zero point energy are 10 kcal mol^{-1} for $HCl^\dagger + Na$; and 18 kcal mol^{-1} for $HF^\dagger + Na$; with zero point energies included the corresponding figures are $4.2 \text{ kcal mol}^{-1}$ and 12 kcal mol^{-1} .

The ratio $-\Delta I(v, J)/I(v, J)$ was the ratio of the change in population to the total population, $-\Delta N(v, J)/N(v, J)$, which in turn was equal to the endothermic rate constant for reaction $k(v, J)$.^{4(b)} Averaging over the first five to eight J levels in each reactive v level gave the endothermic rate constant $k_{\text{endo}}(v)$. For further details, see Ref. 4(b).

To obtain populations $N(v, J)$, the signals $I(v, J)$ were multiplied by the factor T/A , where T is the transmissivity of the spectrometer-plus-detector system, and A is the Einstein transition probability for spontaneous emission. The transmissivity was obtained by recording a black body spectrum over the wavelength region used in the experiment, and comparing this to the theoretical black body emission calculated for the same temperature. The A factors were taken from Ref. 31.

The signals from the lock-in amplifiers were digitized and recorded by an on-line minicomputer. This computer was later used to deconvolute overlapped peaks by a least-squares filtering technique.

III. RESULTS AND DISCUSSION

A. Vibrational dependence of reaction rates

Reactions (1) and (2) are both endothermic (Fig. 2) and consequently a reaction threshold is expected; for vibrational levels below the endothermicity insignificant reaction should occur. The mean temperature weighted according to reagent masses³² is $T_{\text{trans}}^\circ = 940 \text{ K}$ [see Eq. (9) below], hence 10^{-1} of the collisions have sufficient

thermal energy to surmount the barrier for the $HCl + Na$ reaction, and 10^{-3} could surmount the barrier for the $HF + Na$ reaction. For Reaction (1) ($HCl + Na$) $v=1$ has sufficient energy to react, and so depletion from all four v levels populated by the prereaction (PR-3) is expected. The results are displayed in Fig. 3. The top panel shows the vibrational distribution of HCl from the prereaction and the bottom panel shows the (relative) endothermic rate constants for Reaction (1) as a function of the HCl vibrational quantum number. Despite the markedly different distributions of HCl (top panel) the rate constants for reaction all agree to within experimental error. All levels are reactive. To the accuracy of this data the rate increases linearly for additions of (vibrational) energy above threshold.

The results for the reaction of HF with Na [Reaction (2)] are displayed in Fig. 4. Again, the top panel shows the HF vibrational distributions from the prereactor while the bottom panel shows the relative endothermic rate constants. In this case, $v=1$ does not have sufficient energy to surmount the endothermic barrier. The experiments show that $v=1$ does not react: there was no population change for $v=1$ (for any prereaction). The reaction then began at $v=2$ and increased until $v=5$. The reason for the dip at $v=6$ is not known. There is no reason to expect the reaction rate to decrease for $v=6$ and it would appear that there was some other effect responsible.

This same anomaly was observed previously in the "covalent" endothermic reactions $HF + Cl$, Br ^{4(b)}; it

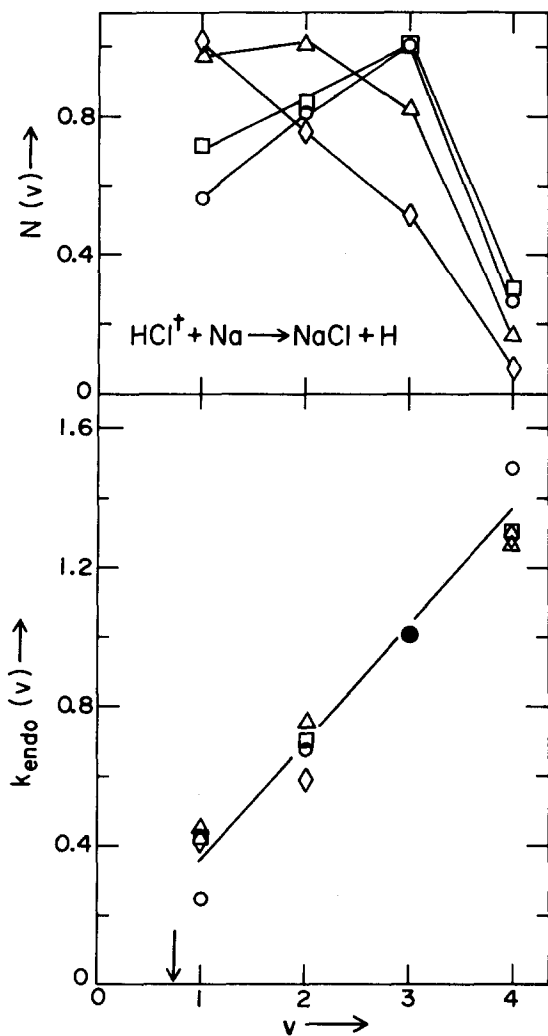


FIG. 3. Top panel: the vibrational distribution of HCl from the prereaction ($\text{Cl} + \text{HI}$; PR-3). Bottom panel: relative endothermic rate constant $k_{\text{endo}}(v)$. The arrow on the bottom scale marks the reaction threshold. Symbols are identified in Table I.

only occurred for $v=6$ of HF produced by the prereaction $\text{F} + \text{HI}$ (PR-2). It was independent of HI flow rate and the prereactor geometry, and consequently independent of the degree of relaxation of the HF. The deviation of this $v=6$ reading suggests smaller depletion than expected—either because the rate of reaction is less than that for $v=5$ (which theory does not support¹¹), or more likely because some $\text{HF}(v=6)$ is formed when the atomic beam (halogen atom or alkali metal) is “on,” thus causing enhancement of the $\text{HF}(v=6)$ signal which evidences itself as a diminished fractional decrease.

Rotational relaxation within the v level does not explain this anomaly. If this process were responsible all v levels, above and below threshold, would show this effect, whereas only $v=6$ shows it. Rotational relaxation, moreover, is least likely to affect $v=6$ since this level is only sparsely populated at high J ($J=10$ has been observed in initial-distribution work³³ and $J=6-7$ in the more relaxed distributions obtained here) and consequently there is very little to relax into the lower J

levels. If all levels *except* $v=6$ were affected by rotational relaxation this would lower the fractional depletion observed from these levels relative to $v=6$, which is the opposite to what is observed. We have, in addition, good evidence that rotational relaxation by the atomic species is insignificant.⁵ Any explanation must take into account that the small unexplained contribution to $v=6$ occurs only when the depleting atomic species is “on.” It should also be noted that no such anomaly exists for the depletion of the highest v level of HCl. In sum, we have no explanation for the anomalously low fractional depletion of $\text{HF}(v=6)$; it appears to be peculiar to the prereaction $\text{F} + \text{HI}$.

The increase in endothermic rate constant from $v=2$ to $v=5$ of HF and from $v=1$ to $v=4$ of HCl [Reactions (1) and (2)] is the principal finding from the present work. These increases in relative rate constant are consistent with those obtained for covalent endothermic reactions [e.g., $\text{HF}^\dagger + \text{Cl}$, see Ref. 4(b)].

The fractional changes do not—without further calibration—give any information about the absolute magnitude of the rate. Absolute reactive cross sections must be estimated by independent methods (see below). The increase in rate constant for a small increment of energy which takes the system from just below the barrier to just above is not available from this work, since there was no depletion observed for the level (for

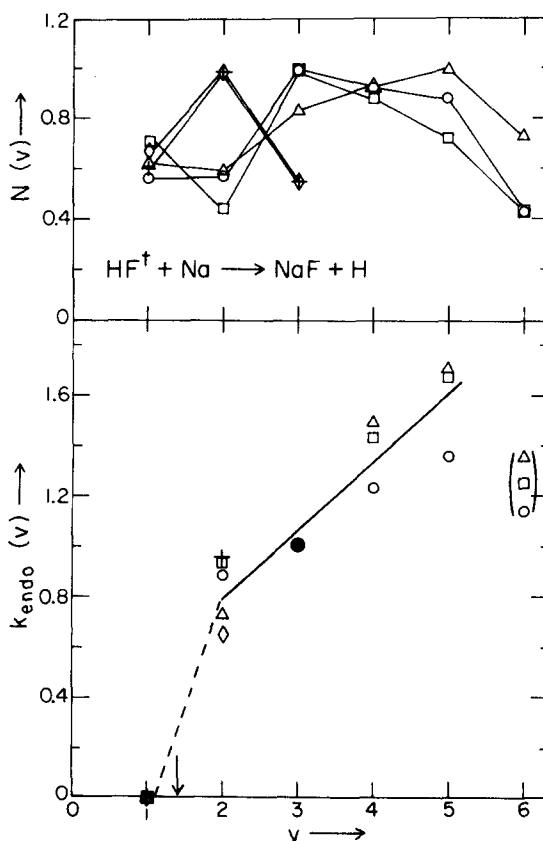


FIG. 4. Top panel: the vibrational distribution from the prereactions $\text{F} + \text{H}_2$ and $\text{F} + \text{HI}$ (PR-1, PR-2 as well as $\text{F} + \text{CH}_3\text{I}$). Bottom panel: relative endothermic rate constant, $k_{\text{endo}}(v)$. The arrow on the bottom scale marks the reaction threshold. Symbols are identified in Table I.

HF + Na) below threshold. This increase has been shown to be large in other work involving hydrogen halide plus alkali metal.¹⁸

The fact that the $v=1$ level of HF showed no depletion due to the presence of Na supports the conclusion that the depletions that we observe are due to reactive encounters rather than deactivation effects. If deactivation were important—e.g., if Na gave rise predominantly to vibrational deactivation of HF—then molecules would tend to accumulate in $v=1$ since the vibrational distributions coming from the prereactor have populations in the higher v levels that are greater than the population in $v=1$, and the probability of collisional deactivation is known to be greater for higher v levels. No enhancement of the $v=1$ population is observed.

B. Cross section for HF[†]($v=5$) + Na

The rate constants displayed in Figs. 3 and 4 have been normalized to an arbitrary v level ($v=3$). These depletions can be put on an absolute scale. In this work the reactive cross section for HF($v=5$) has been obtained by several (approximate) methods.

The first method involved comparing the rate of HF[†] + Na with the rate of a reaction of known cross section.

The reaction chosen was



which has a measured cross section of 5 \AA^2 .³⁴ Since it was not possible to measure the rate of formation of product (NaI or CH₃) a method was devised to obtain the rate of removal of CH₃I. It was found possible to use CH₃I as the molecular prereagent to form HF[†] by reaction with F atoms, viz.,

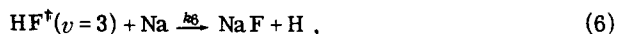


Hence HF[†] became the "indicator" of CH₃I concentration. Since HF[†]($v>1$) can react with Na [by Reaction (2)] only HF[†]($v=1$) was used as indicator. Depletion of HF[†]($v=1$) must be due to a removal of CH₃I by Reaction (3). Conditions had to be chosen so that comparable amounts of Reactions (3) and (4) took place in the low pressure region below the prereactor. This was achieved by having the molecular prereagent injector tip extend ~ 2 mm below the bottom of the prereactor.

Immediately prior to using CH₃I as the molecular prereagent, H₂ was used as a "control" (i.e., PR-1). When HF[†] was formed in this prereaction no depletion of HF[†]($v=1$) was observed. However, with CH₃I as the prereagent, HF[†]($v=1$) was depleted by $\sim 4\%$. An analysis of the kinetic equations, assuming that removal at the cold walls is the dominant process for disappearance of HF[†], yielded the result (see Appendix)

$$\frac{\Delta N/N(v=3) - \Delta N/N(v=1)}{\Delta N/N(v=1)} = \frac{k_6}{k}, \quad (5)$$

where k_6 is the rate constant for the reaction



and k the rate constant for (3). The required fractional depletions were measured.

The rate constant is related to the cross section by

$$k = \sigma \langle v \rangle, \quad (7)$$

where σ is the reactive cross section and $\langle v \rangle$ is the mean collision velocity.³² The collision velocity can be calculated from

$$\frac{1}{2} \mu \langle v \rangle^2 = 2RT_{\text{trans}}^\circ \quad (8)$$

where μ is the reduced mass of the reactant particles, R the gas constant, and T_{trans}° the temperature of the colliding species. The temperature can be calculated from

$$T_{\text{trans}}^\circ = \mu(T_{\text{Na}}^\circ/m_{\text{Na}} + T_{\text{CH}_3\text{I}}^\circ/m_{\text{CH}_3\text{I}}), \quad (9)$$

where T_i° is the temperature of the beam of mass m_i .

This can be simplified to give the velocity

$$\langle v \rangle = [4R(T_{\text{Na}}^\circ/m_{\text{Na}} + T_{\text{CH}_3\text{I}}^\circ/m_{\text{CH}_3\text{I}})]^{1/2}. \quad (10)$$

It is then straightforward to calculate the mean velocity, since the individual temperatures of the intersecting beams are known.

The cross section for the reaction of Na + CH₃I [i.e., (3)] has been measured, but only at one temperature. The experiment reported here was made at a higher temperature. The temperature difference was not large; 570 K³⁴ compared with 940 K for this work. These temperatures correspond to mean translational energies of ~ 1 and 2 kcal mol^{-1} , and hence are in the range where the reactive cross section for Na + CH₃I increases as a function of translational energy.³⁵ A simple method of estimating the increase in cross section is to use the Arrhenius equation

$$k = A \exp(-E_a/RT^\circ) \quad (11)$$

where k is the rate constant for the reaction at temperature T° (K), E_a the activation energy (kcal mol^{-1}), and R the gas constant. A value for the preexponential factor A , typical of the reactions of alkali metal atoms with methyl halides has been given³⁶ as $\log A = 14.63$. The mean velocity can be calculated from the beam parameters given in Ref. 34 by using Eq. (10), and combined with the measured cross section to give k by using (7). With this value for A , the activation energy was calculated to be 3 kcal mol^{-1} . The cross section determined by Eq. (11) for $E_a = 3 \text{ kcal mol}^{-1}$ was 13 \AA^2 , at the temperature of 940 K for the experiment reported here (compared with 5 \AA^2 measured at 570 K³⁴). As a check the 940 K cross section was also calculated from the 570 K value using a hard-sphere model due to Shin.³⁷ The method has been shown to work well for reactions of alkali metal atoms with CH₃I. In the present case it yields [through Eq. (8) of Ref. 37(a), and the hard-sphere diameters in Ref. 37(c)] 11 \AA^2 for Na + CH₃I at our T_{trans}° .

Using 12 \AA^2 for S_r of Na + CH₃I we obtain, by Eq. (5), $S_r = 17 \text{ \AA}^2$ for HF[†]($v=3$) + Na. The depletion for $v=5$ was 1.6 times that of $v=3$, and the cross section for HF[†]($v=5$) + Na was therefore estimated to be $30 \pm 15 \text{ \AA}^2$.

A second method for obtaining a value for the cross section of HF[†] + Na depended on comparison of the rate of this reaction with the known rate for the reaction,



as evidenced by the observed fractional depletion of HF in each case. The rate constant for (12) has been measured to be $2.1 \times 10^{13} \text{ cm}^3 \text{ mol}^{-1} \text{ s}^{-1}$.³⁸ Using Eqs. (7) and (10), the cross section for reaction (12) can therefore be calculated. The observed depletions are related to the cross sections by

$$\frac{\Delta N/N(\text{Na} + \text{HF})}{\Delta N/N(\text{D} + \text{HF})} = \frac{k_{6f_{\text{Na}}}}{k_{12f_{\text{D}}}} \quad (13)$$

$$= \frac{\sigma_{\text{Na+HF}}(v)f_{\text{Na}}}{\sigma_{\text{D+HF}}(v)f_{\text{D}}},$$

where f_x is the flow rate of species x . The Na flow rate was estimated (above) to be $10\text{--}15 \mu\text{mol s}^{-1}$. The D flow rate was not measured directly,³⁹ but the flow of D_2 was $50 \mu\text{mol s}^{-1}$ and assuming 40% dissociation we obtain a D flow rate of $40 \mu\text{mol s}^{-1}$. Substituting these values, with the measured depletions (13% for Na + HF and 2.5% for D + HF) gives a cross section of 33 \AA^2 , for $\text{HF}^\dagger(v=3) + \text{Na}$. The depletion of $\text{HF}^\dagger(v=5)$ is 1.6 times that of $v=3$ and the cross section for $v=5$ is then $50 \pm 30 \text{ \AA}^2$.

A third estimate of the cross section for $\text{HF}^\dagger + \text{Na}$ was obtained using the same method as above, but in this case the comparison reaction was $\text{HF}^\dagger + \text{Cl} \rightarrow \text{HCl} + \text{F}$ which had previously been studied by Douglas *et al.*^{4(b)} The depletion in these experiments was roughly $5\% \pm 3\%$ at a Cl_2 flow rate of $240 \mu\text{mol s}^{-1}$; the Cl flow rate was estimated to lie within the limits $125 \pm 50 \mu\text{mol s}^{-1}$. The cross section for this reaction is $\sim 1 \text{ \AA}^2$. Using an equation similar to (13), the cross section for $\text{HF}^\dagger(v=5) + \text{Na}$ is in the region of $50 \pm 40 \text{ \AA}^2$.

The cross section from these three estimates weighted to favor the better values from methods 1 and 2, is then $50 \pm 30 \text{ \AA}^2$ for $\text{HF}^\dagger(v=5) + \text{Na}$.

The striking feature of this cross section is that it is indicative of highly efficient utilization of reagent vibration in giving rise to endothermic reaction. The mean energy present as translation in the reagents is $\sim 2 \text{ kcal mol}^{-1}$ and that in rotation is $\sim 2 \text{ kcal mol}^{-1}$. Since the vibrational energy for $\text{HF}^\dagger(v=5)$ is $51.8 \text{ kcal mol}^{-1}$ in excess of the zero point energy we conclude that for $\text{HF}^\dagger(v=5) + \text{Na}$ reaction takes place at every gas kinetic collision when $\sim 93\%$ of the reagent energy is present as vibration.

It is also noteworthy that the reactive cross section exceeds by an order of magnitude the (large) cross section of $S_r = 1\text{--}4 \text{ \AA}^2$ obtained in earlier work for endothermic reactions $\text{HX}^\dagger + \text{Y}$ (e. g., $\text{HF}^\dagger + \text{Cl}$)⁴ in which the reagent energy was also present very largely as vibration. The salient difference is believed to be the fact that the present reactions, unlike those studied earlier, involve a switch from a covalent bond in HX to an ionic bond in Na^+X^- . The cross section determined here is marginally greater than the cross section for the slightly endothermic reaction $\text{HCl}^\dagger(v=1) + \text{K}$, which has $S_r \approx 20 \text{ \AA}^2$.¹⁸

The reactions of alkali metal atoms with vibrationally excited hydrogen halides may usefully be described in terms of the "harpooning" model.^{40,41} According to this model the alkali metal atom M "throws out" its valence

electron to the hydrogen halide and pulls in the halogen atom X, by the Coulombic force of attraction. The approximation is made that the London exchange forces operating between M and X can be neglected for reactions of large cross section.

The maximum separation r_c at which the alkali metal can transfer its valence electron to the hydrogen halide is related to the ionization potential of the alkali atom IP and to the electron affinity of the hydrogen halide EA by

$$e^2/r_c \approx \text{IP}(\text{M}) - \text{EA}(\text{HX}), \quad (14)$$

where e is the electron charge.⁴² The reactive cross section is then given by $S_r = \pi r_c^2$.

The ionization potential of Na is well known ($119 \text{ kcal mol}^{-1}$). The electron affinity of HF is not known, but may be obtained from an approximate formula, given by Herschbach,⁴²

$$\text{EA}(\text{HF}) \approx \text{EA}(\text{F}) - D(\text{HF}), \quad (15)$$

where $D(\text{HF})$ is the HF dissociation energy. The equation assumes that the covalent curve is approximately flat in the region where it crosses the ionic bound state. The electron affinity of F is 82 kcal mol^{-1} . The dissociation energy of HF to be used in the case that we wish to estimate EA of HF in vibrational level v , $\text{EA}[\text{HF}(v)]$, is the energy required to reach the dissociation limit from level v ; $D^\circ(v)$. From $v=5$, $D^\circ(v) = 83 \text{ kcal mol}^{-1}$, hence $\text{EA}[\text{HF}(v=5)] = -1.16 \text{ kcal mol}^{-1}$ (a negative electron affinity betokens repulsion). The value of r_c is then calculated to be 2.76 \AA from which the cross section is 24 \AA^2 . This value is lower than the 50 \AA^2 obtained above, but lies within the broad error limits.

The cross section for $v=3$ calculated by the same harpooning model is 17.8 \AA^2 , so that the increase in cross section in going from $v=3$ to $v=5$ is predicted to be 1.3 times, which is (perhaps by chance) in satisfactory agreement with the experimental value of 1.6.

The electron affinity of HF may also be estimated from an *ab initio* calculation.⁴³ The potential curves for HF and HF^- are presented in a figure in this reference. By measuring the separation between an HF v level and the (repulsive) HF^- curve (the vertical electron affinity) it is possible to obtain an estimate of $\text{EA}[\text{HF}(v)]$. The electron affinity for HF($v=5$) obtained in this fashion is $-11.5 \text{ kcal mol}^{-1}$ as compared to $-1.16 \text{ kcal mol}^{-1}$ calculated from (15). The effect on the harpooning cross section of this decreased electron affinity is small; the calculated cross section drops to 20 \AA^2 , as compared to 24 \AA^2 from the first calculation.

The harpooning separation $r_c (= 2.76 \text{ \AA}$ for $v=5$ of HF) is sufficiently small that changes in energy of the covalent curve with internuclear separation cannot properly be ignored. Nonetheless, the electron-jump model may have sufficient validity to provide a cross section within a factor of 2, and also to shed some light on the effect of increased vibrational excitation in the molecule under attack. Recently, Wu⁴⁴ reported the results of the calculation of potential energy barriers for the reactions of $\text{M} + \text{CH}_3\text{X}$ ($\text{M} = \text{Rb}, \text{K}; \text{X} = \text{I}, \text{Br}$) by the harpooning

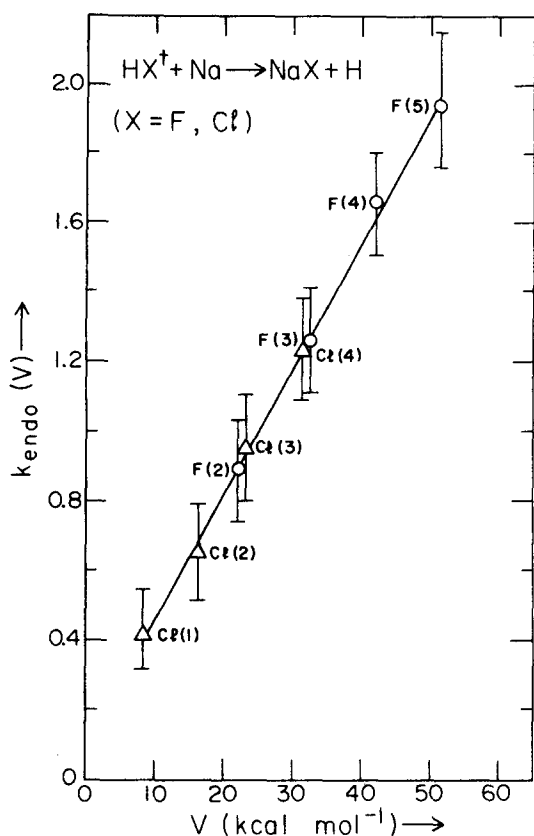


FIG. 5. Comparison of the reactions $\text{HCl} + \text{Na}$ (1) (Δ) and $\text{HF} + \text{Na}$ (2) (\circ). The curves are plotted on the basis that the reactive cross section for $\text{HCl}(v=4)$ is the same as that of $\text{HF}(v=3)$; see text. The error bars are one standard deviation of the scatter of the points from Figs. 3 and 4. Points labeled $F(v)$ refer to reaction by HF in level v , and similarly $\text{Cl}(v)$ refers to reagent HCl in level v .

model. Good agreement was obtained between these calculated results and experimental data on translational energy thresholds. The crossing from the covalent to the ionic potential took place over the range $r_c = 3.1\text{--}3.3 \text{ \AA}$.

C. Comparison of $\text{HF}^\dagger + \text{Na}$ and $\text{HCl}^\dagger + \text{Na}$

The depletions shown in Figs. 3 and 4 are on (separate) relative scales, and direct comparison between the two is not possible. However by measurement of the actual depletions in experiments performed directly following one another, with unchanged reagent flows, it was possible to determine that the depletion for $\text{HCl}(v=4)$ was approximately equal to that for $\text{HF}(v=3)$. While the quantum numbers are different, the corresponding vibrational energies are approximately the same in the two cases— $31.52 \text{ kcal mol}^{-1}$ for $\text{HCl}(v=4)$ and $32.52 \text{ kcal mol}^{-1}$ for $\text{HF}(v=3)$. This connects the two experimental systems. The cross section for $\text{HCl}(v=4)$ is then estimated to be $35 \pm 20 \text{ \AA}^2$. The depletions, normalized to the same vibrational energy, are given in Fig. 5. The figure shows that the reactive cross sections rise at approximately the same rate. In addition, the same absolute vibrational energy in HX^\dagger gives rise to the same absolute cross-section for reaction, irrespective of whether $X = \text{Cl}$ or F . On the other hand, if the depletions

are plotted in a scaled fashion as a function of the vibrational energy *in excess of the barrier height*, the curve for (1) ($\text{HCl}^\dagger + \text{Na}$) is lower than, but parallel to, the curve for (2) ($\text{HF}^\dagger + \text{Na}$) (Fig. 6); i.e., a given vibrational energy in excess of the barrier gives rise to a larger reactive cross section for $\text{HF}^\dagger + \text{Na}$ than for $\text{HCl}^\dagger + \text{Na}$.

The electron-jump model together with Eq. (15) (which is approximate) predicts that a given absolute vibrational energy in HCl^\dagger will give rise to a larger EA than the same energy in HF^\dagger ; consequently for $\text{HCl}(v=4) + \text{Na}$ the model gives $S_r = 30 \text{ \AA}^2$, whereas for $\text{HF}(v=3) + \text{Na}$ it gives $S_r = 20 \text{ \AA}^2$. Experimentally the reactive cross sections are indistinguishable ($\approx 35 \text{ \AA}^2$).

The contribution of the electron-jump model to our understanding of these findings appears to be twofold. In the first place it provides a rationale for the large reactive cross sections, assuming that HX^\dagger can approach Na to r_c without incurring significant repulsion. (Note that the harpooning model makes assumptions only about the repulsion between HX^\dagger and Na on a vibronic energy surface, rather than the repulsion between HX and Na on the underlying electronic energy surface). Secondly this model gives some insight into the moderate (or negligible) difference in the absolute S_r for $\text{HCl}^\dagger + \text{Na}$ and $\text{HF}^\dagger + \text{Na}$ at a given vibrational energy, V_{reag} . For a given V_{reag} the EA of HCl^\dagger and HF^\dagger are different (for $V_{\text{reag}} = 32 \text{ kcal}$ EA(HCl^\dagger) = 12 kcal mol^{-1} and EA(HF^\dagger) = $-23 \text{ kcal mol}^{-1}$) but the value of r_c is sufficiently insensitive to EA to yield comparable reactive cross sections. The value of r_c [from Eq. (14)] is $r_c = [e^2 / (IP - EA)]$; for $|EA| \ll IP$ this becomes $r_c \approx [e^2 / IP]$.

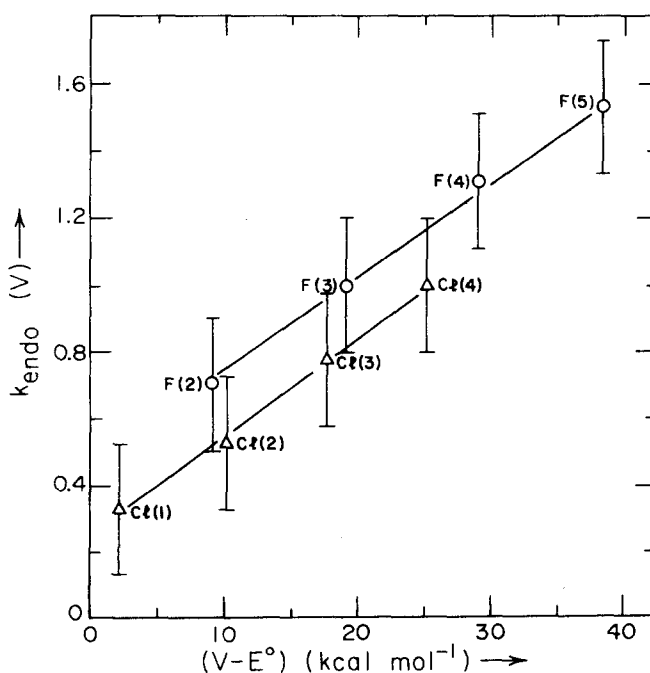


FIG. 6. Comparison of the reaction $\text{HCl} + \text{Na}$ (1) (Δ) and $\text{HF} + \text{Na}$ (2) (\circ). The curves are plotted as a function of the vibrational energy V in excess of that required to cross the barrier E° ; cf. caption to Fig. 4. The symbols $F(v)$ and $\text{Cl}(v)$ have the same meaning as in the previous figure.

The fact that the slopes dS_r/dV_{reag} are indistinguishable for $\text{HCl}^\dagger + \text{Na}$ and $\text{HF}^\dagger + \text{Na}$ can best be understood in the light of the trajectory study which compared various late-barrier-crest potential-energy surfaces (using the mass combination $\text{LH} + \text{H} \rightarrow \text{L} + \text{HH}$ appropriate to $\text{HX} + \text{Na} \rightarrow \text{H} + \text{NaX}$).^{45 (a)} It was found that the slopes dS_r/dV_{reag} differed markedly if (a) the pair of energy surfaces differed in regard to the energy rise along the approach-coordinate and if, at the same time, (b) the collision energy was too small to carry the system up that energy rise. This is easy to understand; vibrational energy in the bond under attack cannot be efficiently utilized if the reactants are unable to approach to within bonding distance.

Since in the present experiments we observe that dS_r/dV_{reag} is the same for $\text{HCl}^\dagger + \text{Na}$ and $\text{HF}^\dagger + \text{Na}$, we conclude either that (a) the pair of energy surfaces have a similar energy rise along the approach coordinate (similar G character, where G is the gradualness of the rise⁴⁵) or (b) that the collision energy is sufficient to render the fraction of the barrier along the approach coordinate irrelevant. In view of the fact that the measured absolute reactive cross sections correspond to reaction at every gas-kinetic collision it would seem that requirement (b) is met, otherwise a significant fraction of collisions would fail to lead to reaction. This carries the further implication that the energy surfaces are S type (a so-called "sudden" rise to the late barrier crest, occurring largely in the exit valley). The mean thermal energy is only ~ 2 kcal mol⁻¹. If this permits the average collision to result in reaction, no more than ~ 2 kcal mol⁻¹ of the endothermic barrier—which has a total magnitude of $E_c = 9.9$ kcal mol⁻¹ for $\text{HCl} + \text{Na}$ and $E_c = 18.4$ kcal mol⁻¹ for $\text{HF} + \text{Na}$ (Fig. 2)—can lie along the coordinate of approach.

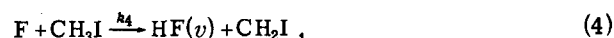
To conclude, the same hypothesis (an S -type late barrier), accords (i) with the observation of large reactive cross section under conditions of low collision energy with enhanced reagent vibration, and also seems to accord (ii) with the observation of indistinguishable slopes dS_r/dV_{reag} for the two systems studied, $\text{HCl}^\dagger + \text{Na}$ and $\text{HF}^\dagger + \text{Na}$.

ACKNOWLEDGMENTS

F. E. Bartoszek and B. A. Blackwell thank the Natural Sciences and Engineering Research Council of Canada for scholarships. We would like to thank Dr. D. Brandt, Dr. R. R. Herm, Professor D. R. Herschbach, Dr. D. M. Manos, and Dr. C. Sholeen for help with the sodium oven design. Special thanks go to R. G. Josephs for skillful construction of the sodium oven. The work described here was supported in part by the Natural Sciences and Engineering Research Council of Canada (NSERC), and in part, by Atomic Energy of Canada Ltd.

APPENDIX

To obtain a relation between the fractional depletions of HF (from the reaction $\text{F} + \text{CH}_3\text{I}$, (4)) and the reactive cross sections, the following kinetic scheme was used. The reactions are



The rate constants k_4 and k_2 are specific to the vibrational level v , but the explicit dependence will be suppressed for convenience.

The steady-state equation for HF is

$$\begin{aligned} d/dt. [\text{HF}(v)] = & k_4[\text{F}][\text{CH}_3\text{I}] - k_2[\text{Na}][\text{HF}(v)] \\ & - k_p[\text{HF}(v)], \end{aligned} \quad (A1)$$

where k_p is the rate of pumping—assumed to be the same for all species. The steady-state concentration of HF is

$$[\text{HF}(v)] = k_4[\text{F}][\text{CH}_3\text{I}]/(k_2[\text{Na}] + k_p). \quad (A2)$$

The concentration of HF in the absence of Na is $[\text{HF}]^\circ$ and is given by

$$[\text{HF}(v)]^\circ = k_4[\text{F}][\text{CH}_3\text{I}]^\circ/k_p, \quad (A3)$$

where the superscript on the CH_3I concentration indicate the concentration in the absence of Na.

The steady state equation for CH_3I is

$$\begin{aligned} d/dt. [\text{CH}_3\text{I}] = & R(\text{CH}_3\text{I}) - k_4[\text{F}][\text{CH}_3\text{I}] \\ & - k_3[\text{Na}][\text{CH}_3\text{I}] - k_p[\text{CH}_3\text{I}], \end{aligned} \quad (A4)$$

from which

$$[\text{CH}_3\text{I}]^\circ = R(\text{CH}_3\text{I})/(k_4[\text{F}] + k_p) \quad (A5)$$

and

$$[\text{CH}_3\text{I}] = R(\text{CH}_3\text{I})/(k_4[\text{F}] + k_3[\text{Na}] + k_p), \quad (A6)$$

where R is the inflow rate of CH_3I , and it is assumed that R is uninfluenced by the presence of Na.

The depletion $\Delta N/N$ of HF is given by

$$\Delta N/N(v) = ([\text{HF}(v)] - [\text{HF}(v)]^\circ)/[\text{HF}(v)]^\circ. \quad (A7)$$

Substituting (A2) and (A3) gives

$$\begin{aligned} \Delta N/N(v) = & \frac{k_4[\text{F}][\text{CH}_3\text{I}]/(k_2[\text{Na}] + k_p) - (k_4[\text{F}][\text{CH}_3\text{I}]^\circ)/k_p}{k_4[\text{F}][\text{CH}_3\text{I}]^\circ/k_p} \\ = & \frac{-k_2[\text{Na}] - k_p\{1 - [\text{CH}_3\text{I}]/[\text{CH}_3\text{I}]^\circ\}}{k_2[\text{Na}] + k_p}. \end{aligned} \quad (A8)$$

Assuming that the rate of cryopumping is the largest rate of removal, i. e., $k_p \gg k_2[\text{Na}]$, gives

$$\Delta N/N(v) = -k_2[\text{Na}]/k_p - \{1 - [\text{CH}_3\text{I}]/[\text{CH}_3\text{I}]^\circ\}. \quad (A9)$$

The ratio of CH_3I concentrations can be obtained using (A5) and (A6) to give

$$[\text{CH}_3\text{I}]/[\text{CH}_3\text{I}]^\circ = (k_4[\text{F}] + k_p)/(k_4[\text{F}] + k_3[\text{Na}] + k_p). \quad (A10)$$

Subtracting both sides (separately) from unity, and assuming that pumping is dominant (i. e., $k_p \gg k_4[\text{F}] + k_3[\text{Na}]$),

$$1 - [\text{CH}_3\text{I}]/[\text{CH}_3\text{I}]^\circ = k_3[\text{Na}]/k_p. \quad (A11)$$

Combining (A9) and (A11) gives the result

$$\Delta N/N(v) = -k_2[\text{Na}]/k_p - k_3[\text{Na}]/k_p. \quad (A12)$$

For $v=1$ of HF (which is endothermic), $k_2(v=1)=0$ and thus

$$\Delta N/N(v=1) = -k_3[\text{Na}]/k_p \quad (\text{A13})$$

Combining (A12) and (A13) for $v=3$ of HF gives Eq. (5) of the text. Note that k_2 here is the same as k_6 , and k_3 the same as k , in the text.

- ¹(a) R. B. Bernstein, *Israel J. Chem.* 9, 615 (1971); (b) J. C. Polanyi, *Acc. Chem. Res.* 5, 161 (1972); (c) V. S. Letokhov, *Science* 180, 451 (1973); (d) J. C. Polanyi and J. L. Schreiber, in *Physical Chemistry—An Advanced Treatise*, Vol. VIA, *Kinetics of Gas Reactions*, edited by H. Eyring, W. Jost, and D. Henderson (Academic, New York, 1974), Chap. 6, p. 383; (e) I. W. M. Smith, in *The Excited State in Chemical Physics*, edited by J. W. McGowan (Interscience, New York, 1975), Chap. 1, p. 1; (f) P. J. Kuntz, in *Dynamics of Molecular Collisions*, Part B, edited by W. H. Miller (Plenum, New York, 1976), Chap. 2, p. 53; (g) R. D. Levine and R. B. Bernstein, in *Dynamics of Molecular Collisions*, Part B, edited by W. H. Miller (Plenum, New York, 1976), Chap. 7, p. 323; (h) R. B. Bernstein, *ACS Symposium Series* 56, edited by P. R. Brooks and E. F. Hayes (American Chemical Society, Washington, 1977), pp. 3–21; (i) J. Wolf- rum, *Ber. Bunsenges. Phys. Chem.* 81, 115 (1977); (j) M. R. Levy, *Reaction Kinetics*, 10 (1–2), pp. 1–252 (1979); (k) I. W. M. Smith, *Kinetics and Dynamics of Elementary Gas Reactions* (Butterworths, London, 1980).
- ²L. T. Cowley, D. S. Horne, and J. C. Polanyi, *Chem. Phys. Lett.* 12, 144 (1971).
- ³A. M. G. Ding, L. J. Kirsch, D. S. Perry, J. C. Polanyi, and J. L. Schreiber, *Faraday Discuss. Chem. Soc.* 55, 252 (1973).
- ⁴(a) D. J. Douglas, J. C. Polanyi, and J. J. Sloan, *J. Chem. Phys.* 59, 6679 (1973) [Part IV of the present series]. (b) *Chem. Phys.* 13, 15 (1976) [Part VI of the present series; this paper references earlier parts of the series].
- ⁵B. A. Blackwell, J. C. Polanyi, and J. J. Sloan, *Chem. Phys.* 30, 299 (1978) [Part IX of the present series].
- ⁶(a) J. C. Polanyi, *J. Chem. Phys.* 31, 1338 (1959); (b) J. C. Polanyi and W. H. Wong, *J. Chem. Phys.* 51, 1439 (1969); (c) M. H. Mok and J. C. Polanyi, *ibid.* 51, 1451 (1969); (d) B. A. Hodgson and J. C. Polanyi, *ibid.* 55, 4745 (1971).
- ⁷(a) K. G. Anlauf, D. H. Maylotte, J. C. Polanyi, and R. B. Bernstein, *J. Chem. Phys.* 51, 5716 (1969); (b) J. C. Polanyi and D. C. Tardy, *ibid.* 51, 5717 (1969); (c) D. S. Perry and J. C. Polanyi, *Chem. Phys.* 12, 419 (1976).
- ⁸D. S. Perry, J. C. Polanyi, and C. W. Wilson, Jr., *Chem. Phys. Lett.* 24, 484 (1974).
- ⁹J. B. Anderson, *J. Chem. Phys.* 52, 3849 (1970).
- ¹⁰R. N. Porter, L. B. Sims, D. L. Thompson, and L. M. Raff, *J. Chem. Phys.* 58, 2855 (1973).
- ¹¹D. S. Perry, J. C. Polanyi, and C. W. Wilson, Jr., *Chem. Phys.* 3, 317 (1974).
- ¹²G. L. Hofacker and R. D. Levine, *Chem. Phys. Lett.* 9, 617 (1971).
- ¹³J. W. Duff and D. G. Truhlar, *J. Chem. Phys.* 62, 2477 (1975).
- ¹⁴(a) J. C. Polanyi and N. Sathyamurthy, *Chem. Phys.* 33, 287 (1978); (b) 37, 259 (1979).
- ¹⁵(a) W. A. Chupka and M. E. Russell, *J. Chem. Phys.* 49, 5426 (1968); (b) W. A. Chupka, *Ion-Molecule Reactions*, edited by J. L. Franklin (Plenum, New York, 1972), Chap. 3.
- ¹⁶P. J. Brown and E. F. Hayes, *J. Chem. Phys.* 55, 922 (1971).
- ¹⁷P. J. Kuntz and W. N. Whitton, *Chem. Phys. Lett.* 34, 340 (1975).
- ¹⁸(a) T. J. Odiorne, P. R. Brooks, and J. V. V. Kasper, *J. Chem. Phys.* 55, 1980 (1971); (b) J. G. Pruett, F. R. Grabiner, and P. R. Brooks, *ibid.* 63, 3335 (1974); (c) J. G. Pruett, F. R. Grabiner, and P. R. Brooks, *ibid.* 63, 1173 (1975).
- ¹⁹Y. Zeiri and M. Shapiro, *Chem. Phys.* 31, 217 (1978).
- ²⁰M. Shapiro and Y. Zeiri, *J. Chem. Phys.* 70, 5264 (1979).
- ²¹G. G. Balint-Kurti and R. N. Yardley, *Faraday Discuss. Chem. Soc.* 62, 77 (1977); M. M. L. Chen and H. F. Schaefer III, *J. Chem. Phys.* 72, 4376 (1980).
- ²²A. Gupta, D. S. Perry, and R. N. Zare, *J. Chem. Phys.* 72, 6237 (1980); 72, 6250 (1980).
- ²³Z. Karny and R. N. Zare, *J. Chem. Phys.* 68, 3360 (1978).
- ²⁴J. C. Tully, "Semi-empirical diatomics-in-molecules potential energy surfaces," in *Potential Energy Surfaces*, edited by K. Lawley, *Adv. Chem. Phys.* Vol. XLII (1980), p. 63.
- ²⁵B. A. Blackwell, J. C. Polanyi, and J. J. Sloan, *Faraday Discuss. Chem. Soc.* 62, 147 (1977).
- ²⁶J. C. Polanyi and K. B. Woodall, *J. Chem. Phys.* 57, 1574 (1972).
- ²⁷(a) B. A. Blackwell, M. Sc. thesis, University of Toronto, 1978; (b) D. J. Douglas, Ph.D. thesis, University of Toronto, 1976; (c) K. B. Woodall, Ph.D. thesis, University of Toronto, 1971.
- ²⁸(a) H. L. Welsh, C. Cumming, and E. J. Stansbury, *J. Opt. Soc. Am.* 41, 712 (1951); (b) H. L. Welsh, E. J. Stansbury, J. Romanko, and T. Feldman, *J. Opt. Soc. Am.* 45, 338 (1955).
- ²⁹C. Sholeen, Ph.D. thesis, University of California, Berkeley, 1976.
- ³⁰F. E. Bartoszek, Ph.D. thesis, University of Toronto, 1979.
- ³¹(a) R. N. Sileo and T. A. Cool, *J. Chem. Phys.* 65, 117 (1976); (b) J. M. Herbelin and G. Emanuel, *ibid.* 60, 689 (1974).
- ³²J. C. Polanyi, J. J. Sloan, and J. Wanner, *Chem. Phys.* 13, 1 (1976).
- ³³L. W. Dickson, L. N. Y. Kwan, and J. C. Polanyi, *Chem. Phys.* (to be published).
- ³⁴J. H. Birely, E. A. Entemann, R. R. Herm, and K. R. Wilson, *J. Chem. Phys.* 51, 5461 (1969).
- ³⁵M. E. Gersh and R. B. Bernstein, *J. Chem. Phys.* 55, 4661 (1971); 56, 6131 (1972).
- ³⁶A. F. Trotman-Dickenson, *Gas Kinetics* (Butterworths, London, 1955).
- ³⁷(a) H. K. Shin, *Chem. Phys. Lett.* 34, 546 (1975); (b) 38, 253 (1976); (c) 45, 533 (1977).
- ³⁸J. F. Bott and R. F. Heidner, *J. Chem. Phys.* 68, 1708 (1978).
- ³⁹F. E. Bartoszek, D. M. Manos, and J. C. Polanyi, *J. Chem. Phys.* 69, 933 (1978).
- ⁴⁰R. A. Ogg, Jr. and M. Polanyi, *Mem. Proc. Manchester Lit. Philos. Soc.* 78, 41 (1934); *Trans. Faraday Soc.* 31, 604, 1375 (1935).
- ⁴¹J. L. Magee, *J. Chem. Phys.* 8, 687 (1940).
- ⁴²D. R. Herschbach, in *Molecular Beams*, edited by J. Ross (Interscience, New York, 1966), p. 319.
- ⁴³V. Bondybey, P. K. Pearson, and H. F. Schaefer, *J. Chem. Phys.* 57, 1123 (1972).
- ⁴⁴K. T. Wu, *J. Phys. Chem.* 83, 1043 (1979).
- ⁴⁵(a) J. C. Polanyi and N. Sathyamurthy, *Chem. Phys.* 33, 287 (1978); (b) 37, 359 (1979).